Noname manuscript No.
(will be inserted by the editor)

ENSO influence on the North Atlantic European climate: A non-linear and non-stationary approach

Jorge López Parages · Belén Rodríguez-Fonseca · Dietmar Dommenget · Claudia Frauen

Received:xx / Accepted:xx / Published online:xx

Abstract El Niño Southern Oscillation (ENSO) impact on the North Atlantic European sector (NAE) is still under discussion. Recent studies have found a non stationary feature of this teleconnection, suggesting an effective modulating role of the ocean mean state. Nevertheless, physical explanations about the underlying mechanisms have been little studied in the available literature. In addition, ENSO events show different SST spatial patterns, phases, and amplitudes, which can also influence on the related remote impacts. In view of all this, in the present study a set of partially coupled experiments have been performed with a global atmospheric general circulation model in which different SST ENSO patterns are superimposed over distinct Pacific and Atlantic SST mean states. These SST background conditions are constructed according to the observational difference between periods with a distinct impact of ENSO on the leading Euro-Mediterranean rainfall mode in late winter-early spring. Our results point to two distinct mechanisms associated with ENSO that can be modulated by the SST mean state: 1) the thermally driven direct circulation (Walker and Hadley cells) connecting the Atlantic and Pacific basins, and 2) the Rossby wave propagation from the tropical Pacific to the North Atlantic. The former elucidates that the positive NAO-like pattern usually related to La Niña events could be only valid for selected decades. The latter explains a reinforced signature of Eastern Pacific Niños on the Euro-Mediterranean rainfall when the tropical Pacific is warmer than usual and the North Atlantic is colder than usual. This feature is consistent with the changing ENSO impact identified in previous studies and demonstrates how the ENSO teleconnection with the NAE climate at interannual timecales could be modulated by multidecadal changes in the SST. According to our results, the assumption of stationarity which is still common to many studies of ENSO teleconnections clearly has to be questioned.

J. López-Parages
Departamento de Física de la Tierra, Astronomía y Astrofśica I (Geofísica y Meteorología). Instituto de Geociencias UCM-CSIC, Facultad de C.C. Físicas , Universidad Complutense de Madrid (UCM), Pza de las Ciencias, 28040, Spain
Tel.: +0034-91-3944513
E-mail: jlopezpa@ucm.es

1 Introduction

The El Niño-Southern Oscillation (ENSO) is the coupled ocean-atmosphere mode that is considered as the main driver of global atmospheric teleconnections at interannual timescales. Its oceanic component (El Niño), which is characterized by anomalous Sea Surface Temperatures (SSTs) over the equatorial Pacific Ocean, alters the sources of atmospheric heating and, as a consequence, affects remote regions around the globe. During El Niño (La Niña) events the central-eastern tropical Pacific becomes warmer (colder) and the related atmospheric convection and rainfall are shifting along with the anomalous temperature. ENSO related changes in the local divergent flow induce further changes in the divergent and non-divergent (or rotational) flow, therefore impacting distant areas through different teleconnection mechanisms. In the last decades a series of publications have found a non-linear response of zonal winds in the central Pacific to SST anomalies (Kang and Kug, 2002; Philip and van Oldenborgh, 2009; Frauen and Dommenget, 2010). This feature could be associated with two distinct and documented El Niño patterns, Eastern Pacific (EP) and Central Pacific (CP), which have discernibly different impacts on remote regions (Kug et al, 2009; Kao and Yu, 2009; Choi et al, 2011; Frauen et al, 2014). However, whilst the ENSO signature over the Pacific and the tropics has been highly analyzed, ENSO response over extratropical regions requires further investigation. One of the less understood teleconnections is the one associated with the North Atlantic European Sector (NAE), which even is far from being unequivocally accepted (Brönnimann, 2007 and paper therein).

The divergent flow response associated with ENSO involves 1) changes in the Hadley and Walker cells in relation to variations in the convection (Wang, 2002b; Wang and Enfield, 2003; Wang and Picaut, 2004; Ruiz-Barradas et al, 2003) but also 2) changes in the rotational flow by the modification of the planetary vorticity and hence, the triggering of Rossby waves (Cassou and Terray, 2001; Honda et al, 2001).

Regarding the changes in the direct circulation, six centers of action of velocity potential appear when an ENSO episode occurs: three over the equator (western Pacific, eastern Pacific, and Atlantic) and three over mid-latitude regions (west Pacific, near Caribbean Sea, and Europe). These divergent and convergent centers along the globe represent a weakening (for El Niño; strengthening for La Niña) of the Pacific and Atlantic Walker circulations (equatorial centers), and its related Hadley cells in the subtropics (Wang, 2002a; Wang and Picaut, 2004). Thus, climate variability over the NAE could be significantly linked (or not) with tropical Pacific SSTs depending on the intensity and spatial configuration of the previously mentioned anomalous circulations.

Regarding the changes in the rotational flow, the most accepted dynamical mechanism explaining the ENSO-NAE teleconnection via the troposphere implies the disturbance of the Aleutian low through variations in the Pacific Hadley circulation in early and mid winter, and then the downstream propagation of Rossby wavetrains across North America from January (Honda et al, 2001; Moron and Gouirand, 2003). From this month the canonical Tropical Northern Hemisphere Pattern (TNH), which is organized in three centers of actions along the North Pacific-American sector (Mo and Livezey, 1986; Barnston and Livezey, 1987; Livezey and Mo, 1987; Trenberth et al, 1998), is completely established (Bladé et al, 2008), together with a split of the Rossby wavetrain impacting Eura-

sia (Karoly et al, 1989). The resultant rotational atmospheric response to ENSO is formed by a TNH-like pattern and the abovementioned split of the wavetrain, revealing a quasi barotropic structure, and representing the leading rotational mode of upper level streamfunction in the NAE (García-Serrano et al, 2011).

It is worth to highlight that the ENSO atmospheric signal detection in NAE is difficult due to the fact that the atmospheric interannual variability over this region is highly dominated by internal processes (Trenberth et al, 1998; Quadrelli and Wallace, 2002). Nevertheless, the above mentioned studies together with other statistical analyses point to a robust ENSO response (Brönnimann, 2007), which is seasonal dependant (Moron and Gouirand, 2003; Mariotti et al, 2002), maybe nonlinear (Wu and Hsieh, 2004; Pozo-Vázquez et al, 2005a), and possibly nonstationary in time (Knippertz et al, 2003; Sutton and Hodson, 2003; Gouirand and Moron, 2003; Greatbatch et al, 2004), with the late winter being the more appropriate season for finding a robust signal (Brönnimann, 2007). However, a better understanding of how this link is affected by different phases, spatial patterns, and strengths of ENSO events, is necessary.

Concerning the non-stationary behavior of the response, several studies have found a strong impact of ENSO events over the Euro-Mediterranean rainfall in late winter and early spring during the beginning of the 20th century (1900s-1920s) and after the sixties (1970s-1980s), compared to a weak signal in the decades in between (Mariotti et al, 2002; López-Parages and Rodríguez-Fonseca, 2012). Nevertheless, this changing response is not completely accepted and a clear agreement about the possible underlying mechanism is still needed. Several studies have indicated the importance of a realistic representation of the SST mean state in order to properly reproduce the atmospheric response to SST anomalies (Peng and Whitaker, 1999; Cassou and Terray, 2001). Related to this, in a recent paper López-Parages et al (2014) have attributed the variable ENSO-EuroMediterranean rainfall link to changes in the upper mean flow associated with the multidecadal variability of the SST. Thus, new challenges related to a possible modulation of the already not-completely understood ENSO-NAE teleconnection, appear.

With the aim to shed light on these questions, an atmospheric general circulation model (AGCM) is forced in this work with idealized ENSO SST patterns (of different spatial configurations, strengths, and signs) under distinct ocean background states to test, which of the aforementioned features are determinant to better achieve the changing impact of ENSO events on the European region.

The article is organized as follows. We begin by presenting the data and model simulation used for this study (Section 2). The remote impact of ENSO on the NAE is analyzed in Section 3 for different types of El Niño and La Niña events, paying special attention to the non-linear features. Finally, in Section 4, a brief summary and a discussion are presented.

2 Data and Model

In this work a low resolution version (3.75° x 2.5°) of the atmospheric component of the Australian Community Climate and Earth System Simulator (ACCESS) model (Bi et al, 2013) is used to analyze the role of the ocean mean state as modulator of ENSO teleconnections with the NAE climate in February-March-

April after the mature phase of ENSO events, according to López-Parages and Rodríguez-Fonseca (2012) and López-Parages et al (2014).

The ACCESS Model is made up of the Met Office (UKMO) Unified Model AGCM with Hadley Centre Global Environment Model version 2 (HadGEM2) physics (Davies et al, 2005; Martin et al, 2010; Martin et al, 2011). In the present study this model has been coupled in some specific regions to a simple slab ocean model (Washington and Meehl, 1984; Dommenget and Latif, 2002; Murphy et al, 2004; Dommenget, 2010) letting the SSTs over these regions to respond to the different spatial patterns of SST forcing, which in turn have been defined from HadISSTs data (Rayner et al, 2003). A flux correction, however, has been required to force the model SSTs to closely follow a reference SST climatology (1950-2010). The sea ice climatology has been also prescribed here from HadISST dataset.

First of all, a set of control simulations, for which the aforementioned reference SST climatology is modified over the Atlantic (40S-80N) and the tropical Pacific (30S-30N) basins, are performed. To this aim, an anomalous SST pattern (Figure 1a) corresponding to the difference between periods with a distinct impact of ENSO on the Euro-Mediterranean rainfall in late winter and early spring (Mariotti et al, 2002; López-Parages and Rodríguez-Fonseca, 2012), is added or subtracted to the reference SST climatology. This pattern (1a), which resembles an Atlantic Multidecadal Oscillation structure (AMO; Knight et al, 2005; Kang et al, 2014), has been only prescribed here over the Atlantic and the tropical Pacific. This has been done in order to take into account, not only the Atlantic SSTs associated with the AMO, but also the AMO signature on the tropical Pacific (Kucharski et al, 2015; Dong et al, 2006), which could influence the processes involved during the ENSO event. Furthermore, to better analyze the influence of the changing SST background state on the ENSO-NAE teleconnection the amplitude of this anomalous SST pattern, has been doubled. The resultant "modified climatologies" (obtained by adding or subtracting Figure 1a with double amplitude to the reference 1950-2010 climatology) are hereinafter referred as P and N, respectively, in accordance to the positive (P) and negative (N) links, between El Niño and rainfall variability in central Europe, identified in López-Parages et al (2014).

Secondly, for these modified climatologies, a series of sensitivity experiments (see Table 1) are performed superimposing different idealized ENSO patterns as defined in Dommenget et al (2013). These patterns (Figures 1b and c), which represent the non-linear spatial structure of ENSO events in an optimal way, have been normalized to have a Niño-3.4 (5S-5N, 120-170W) mean SST anomaly of +1K (for El Niño events) or -1K (for La Niña events), as in Frauen et al (2014). Hereinafter these spatial patterns will be referred as Eastern Pacific (EP) and Central Pacific (CP) ENSO. Note, however, that in these sensitivity experiments performed with an AGCM only the oceanic component of ENSO (El Niño) is prescribed. Outside the Atlantic and the tropical Pacific, the AGCM model is coupled to the simple slab ocean model. All the experiments are performed considering different signs (El Niño and La Niña) and amplitudes (100% and 200%) of ENSO forcing.

The mean response of each sensitivity experiment has been calculated and compared with the other experiments in order to answer different open questions regarding the influence of distinct types of ENSO phases and patterns (El Niño and La Niña; EP and CP) under different ocean mean states (P and N). The significant differences have been evaluated through the non-parametric Wilcoxon-Mann-Whitney test (Wilks, 2011).

Table 1 Overview of the simulations performed in this study. All of them are 50 years long

ENSO amplitude	**SST mean state**			
	P		**N**	
+200%	EP200 P	CP200 P	EP200 N	CP200 N
+100%	EP100 P	CP100 P	EP100 N	CP100 N
Control	P		N	
-100%	-EP100 P	-CP100 P	-EP100 N	-CP100 N
-200%	-EP200 P	-CP200 P	-EP200 N	-CP200 N

However, it is worth to note that the experimental design applied here only allows us to investigate the direct global impacts of tropical Pacific SSTs during ENSO events and does not capture the entire global impact of ENSO. For instance, the ENSO signature over the Tropical North Atlantic, which also influences the ENSO-related atmospheric response over the North Atlantic and Europe (Mathieu et al, 2004; Ham et al, 2014), is not captured here (taking into account that the AGCM is not coupled to the slab ocean model over the Atlantic basin). Thus, the present study is designed only in order to isolate the direct link between tropical Pacific SSTs during ENSO events and the NAE climate.

A basic observational validation of our experimental results has been also presented in this study. For this purpose, SLP data from NCAR (Trenberth and Paolino, 1980) and from the 20th century reanalysis V2 (20CR; Compo et al, 2011) provided by the NOAA, have been used. The significance of the observational patterns has been also determined by the Wilcoxon-Mann-Whitney test.

3 Results

3.1 ENSO responses under different background climatologies

In this section the anomalous responses, in February-March-April, to distinct ENSO SST patterns (with different signs, amplitudes and spatial patterns) under P and N climatologies, are obtained. The impact is analyzed, for each case, at upper and surface levels, normalizing the ENSO-related patterns by the mean Niño-3.4 SST anomaly values. In order to distinguish the rotational and divergent signals in the upper troposphere, the atmospheric streamfunction and the velocity potential at 200hPa have been presented.

Additionally, the wave activity flux (WAF), which is a vector approximately parallel to the local group velocity of Rossby waves, has been computed directly from the zonally asymmetric part of the anomalous streamfunction regression maps (assuming stationary Rossby waves and neglecting vertical movements; see equation 38 of Takaya and Nakamura 2001 for further details).

3.1.1 EP El Niños

For Eastern Pacific El Niños (EP), the atmospheric response appears stronger in P than in N at upper (Figure 2) and surface (Figure 3) levels. In both cases, the model is able to reproduce the ENSO-related rotational impact over the NAE in late winter and early spring (Gouirand and Moron, 2003; Moron and Plaut, 2003; García-Serrano et al, 2011), that is, a well established TNH pattern together with a significant center located downstream over the European continent. This enhanced signal in P with respect to N is less noticeable when the EP forcing is doubled (Figures 2b,d and 3b,d).

For EP100 El Niños, the intense rotational response in P (Figure 2a) contrasts with the weaker wave activity in N (Figure 2c). This seems to be due to the stronger divergence identified over the tropical Pacific in the former case (see contours in Figures 2a,c), for which the two twin anticyclones straddling the equator and related to the typical Gill-type atmospheric response to equatorial anomalous heating (Gill, 1980), appear also reinforced. Considering that remote impacts associated with tropical convection are sensitive to absolute rather than anomalous values of SST, temperatures required for deep convection (preferentially exceeding a threshold of 26°-28°; see Graham and Barnett 1987) are favored in P mean state, in which the underlying tropical Pacific is warmer (Figure 1a; see also Figure A1 of supplementary material). If EP El Niños are strong (200%) this threshold is exceeded in both, P and N, and so, their related upper level perturbations look similar (Figures 2b,d). Two distinct wavetrains can be clearly identified over the northern hemisphere in those cases in which a strong rotational response is found (in P for normal El EP Niños and in both, P and N, for strong EP El Niños). One is generated from the west Pacific extending east across the North Pacific and then south over North America. A second wavetrain originates from the east tropical Pacific and crosses the North Atlantic northward until the British Islands, where it is reflected towards lower latitudes over the Euro-Mediterranean region. The resultant SLP patterns highlights the barotropic nature of the anomalous perturbation (contours in Figures 3a,b,d). As a consequence, a deep low pressure system appears over the British Islands, and a significant impact on European rainfall is found (shaded in Figures 3a,b,d), being similar to the ENSO-related impact identified in previous studies (Moron and Gouirand, 2003; Bulić and Kucharski, 2012). It is interesting to note that, for EP100 in N, the three centres over Florida, the Labrador Strait and, in particular, over the British Islands appear noticeably weakened (Figure 3c). Hence, the significant Euro-Mediterranean rainfall pattern associated with ENSO is not found (Figure 3c). The aforementioned responses are coherent with the distinct ENSO signature on Euro-Mediterranean rainfall identified, for late winter and early spring, before (under a P-like SST mean state configuration) and after (under a N-like SST mean state configuration) the 1920's, and before (under a N-like SST mean state configuration) and after (under a P-like SST mean state configuration) the 1960's (Mariotti et al, 2002; López-Parages and Rodríguez-Fonseca, 2012; López-Parages et al, 2014). It is worth, however, to quantify the amplitude in the response between observational and model impacts. According to López-Parages et al (2014), an anomaly of 8 $mm/month$ is detected for central European rainfall in relation to $1K$ anomalous warming over the tropical Pacific (see Figures 2b and 2d of that paper). By carefully looking at the EP100 ENSO signature on European rainfall in our idealised experiments (Figure 3a), be-

tween 0.4 and $0.5 \cdot 10^{-5} Kg/m^2 s$ anomalous rainfall is obtained on central Europe for $1.3K$ warming in the Niño 3 region (Figure 1b). This implies between 8 and 10 $mm/month/KNino3$, which reflects a slight overestimation of rainfall in the model with respect to the observations. Let us consider, in order to illustrate these magnitudes, the averaged rainfall in FMA for La Coruña (north-western Iberia; data from the Spanish Meteorological Agency) and Paris (data from Météo-France), which corresponds to 83 and 47 $mm/month$, respectively. According to this, an anomalous EP El Niño episode of $1K$ amplitude is related to an enhanced rainfall in these locations of around $10\% - 12\%$ (La Coruña) and $17\% - 21\%$ (Paris).

A closer inspection also reveals a changing response of surface rainfall over the tropical North Atlantic (Figure 3), which seems to be associated with the distinct eastward extension of the divergence flow signal forced by ENSO (contours in Figure 2). Related to this, for EP200 events a significant rainfall impact is found over the whole TNA and the Sahelian region in P (Figure 3b), while the areas with a significant signature are reduced in N (Figure 3d). A similar difference can be observed between EP100P (Figure 3a) and EP100N (Figure 3c). As it was previously noted, the remote impacts associated with tropical convection depend on absolute values of SST. Hence, the aforementioned extension of the divergent flow towards the TNA depends on both, the Pacific SST mean state (P or N), and the intensity of the EP El Niño event. Thus, when a strong EP El Niño happens under a warm Pacific background state (P), the divergent flow over the TNA is highly perturbed (Figure 2b), and a significant impact is found in rainfall (Figure 3b). On the contrary, if a weak EP El Niño happens over a cold Pacific background state (N), the perturbation at upper levels is clearly reduced (Figure 2c), and the rainfall signature over the TNA weakens (Figure 3c). According to this, EP100P (weak EP El Niño plus warm Pacific mean state; see Figures 2a and 3a) and EP200N (strong EP El Niño plus cold Pacific mean state; Figures 2d and 3d) reflect intermediate cases.

3.1.2 CP El Niños

As for EP El Niños, atmospheric response to the Central Pacific El Niños (CP) appears stronger in P than in N (see Figure 4). The main wavetrain associated with the well-known TNH pattern is obtained for both intensities (CP100 and CP200) and ocean mean states (P and N), finding a similar response as for EP events. Nevertheless, the rotational impact over Europe appears weaker and more northerly located than for EP El Niños. At surface, a negative NAO-like pattern emerges (Figure 5), showing different intensities depending on the mean state and, most specially, on the amplitude of the El Niño forcing.

The intensified rotational response of CP Niños in P is explained, as for EP Niños, by the stronger divergence signal over the tropical Pacific (contoured in Figure 4). The divergent response for CP100N (Figure 4c) is, however, not as weak as for EP100N (Figure 2c). This feature is explained by the fact that, in N, the climatological SSTs in the western tropical Pacific (Figure 1a, opposite sign for N periods) are warmer than on the eastern side, which allows the development of deep convection easily in this region if an anomalous warming is superimposed. As a consequence, the rotational signal over the Pacific North American sector is slightly stronger for CP than for EP events (note the stronger Aleutian low in Figure 4 with respect to Figure 2). Over the North Atlantic, on the contrary, a

weakening of the WAF is found for CP in both, P and N. Related to this, the centre of streamfunction over Canada (positive) appears weaker and more zonally elongated than for EP El Niños and so, a totally positive SLP signal is found at high latitudes (Figure 5). This feature is specially marked in N, for which the positive SLP signal is statistically significant (Figure 5c,d). Regarding the divergent flow response (contours in Figure 4), it seems that the eastward extension over the subtropical North Atlantic appears reinforced in P. At surface (Figure 5), however, no clear differences are identified between P and N at subtropical latitudes. On the contrary, the most distinguishable response is obtained in relation to the intensity of the CP event instead of in relation to the background state, finding a significant impact over the Azores region for strong CP El Niños in both, P and N (Figure 5b,d).

A joint analysis of the rotational and the divergent flow is needed to understand this impact at surface levels. According to the results obtained here the shape of the aforementioned centre of streamfunction over Canada (positive), not only produces the high SLPs over the North Atlantic, but also influences the impact over the Azores region through the divergent flow: If this centre appears slightly southeastward elongated towards the subtropical Atlantic (as in P) the Azores high is significantly perturbed only if the divergent impact associated with ENSO is really strong (Figures 4b and 5b); whilst, if this centre is weaker and zonally distributed (as in N), a slight increase of the divergent flow is enough to significantly change the Azores high (Figures 4d and 5d).

Thus, the changing dipole SLP configuration obtained for CP El Niños is broadly explained by: 1) a distinct propagation of stationary Rossby waves and 2) a different eastward extension towards the North Atlantic of the divergent flow signal associated with ENSO.

The aforementioned signatures over the NAE related to CP and EP El Niños resemble the documented responses in relation to "moderate" and "strong" El Niños (Toniazzo and Scaife, 2006), which responds to the fact that the latter are closely associated with the EP pattern prescribed here (see Figure 2 from Frauen et al, 2014).

3.1.3 La Niñas

A first view of the La Niña experiments reveals a weaker response than for El Niño episodes in both, the rotational and the divergent flow (see Figure 6).

A reinforced TNH pattern associated with CP La Niña events is identified in P (Figures 6a,b) compared to N (Figures 6c,d). This fact, which occurs as a consequence of the stronger convergence in the upper troposphere over the tropical Pacific in P, is in agreement with Frauen et al (2014), who found a stronger atmospheric response for the same SST anomalies under a warmer background tropical Pacific (as occurs here in P). The downstream signal over the NAE is much weaker than for El Niño episodes. A significant center of negative streamfunction is found at upper levels over Western Europe (Figures 6a,c), spreading eastward when La Niña amplitude is doubled (Figures 6b,d). A positive center is also obtained at higher latitudes, being situated over the North Atlantic in N (Figures 6c,d), and further east over the Northern Eurasia in P (Figures 6a,b). This feature seems to explain the positive SLP signal identified in N over Iceland and its surrounding

areas (Figures 7c,d), differently from P, for which the SLP anomalies obtained over the same region are negative (Figures 7a,b).

At lower latitudes the stronger convergence detected over the tropical Pacific in P (Figures 6a,b) with respect to N (Figures 6c,d) reinforces the climatological Walker cell connecting the tropical Pacific with the tropical Atlantic. As a consequence, an anomalous divergence is found over the tropical Atlantic in P, which is related to the enhancement of the two twin anticyclones straddling the equator (Figures 6a,b). This stronger inter-basin connection strengthens, in turn, the meridional Hadley cell over the Atlantic basin (Wang, 2002b), favouring therefore the intensification of the Azores high pressure system (Figures 7a,b). In N, on the contrary, the inter-basin connection is much less intense, and the aforementioned perturbation over the Azores is not found (Figures 7c,d).

The aforementioned characteristics are broadly reproduced for EP La Niñas, finding however a weaker impact over the NAE sector than for CP La Niñas (see Figures A2 and A3 of supplementary material).

4 Summary and Discussion

In this study the role of the ocean mean state as a modulator of the ENSO-NAE teleconnection in late winter and early spring (February-March-April) is explored. To this aim, a set of sensitivity experiments, in which a full complexity AGCM is forced with standardised ENSO patterns of different signs and strengths, are performed. These ENSO patterns are, in turn, superimposed over distinct SST background states over the Atlantic and the tropical Pacific basins. These background SST patterns are obtained by adding the difference between the climatologies in those periods, in which the impact of ENSO over the Euro-Mediterranean rainfall is different, to a control climatology (1950-2010).

Regarding El Niño events it has been found that, a wavetrain crossing the North Atlantic north-eastward reaches the European Continent and a significant impact on the Euro-Mediterranean rainfall is obtained, if the anomalous heating occurs in the eastern side of the tropical Pacific (EP Niños). This feature is dependent on the ocean mean state (P or N), specially if the El Niño amplitude is "normal" (100% EP events). According to this, the aforementioned wavetrain associated with normal EP Niños is clearly enhanced when the tropical Pacific SST mean state is warmer than usual and the North Atlantic SST mean state is colder than usual.

If the heating associated with El Niño occurs in the central tropical Pacific (CP El Niños) the wavetrain towards the North Atlantic is more zonally guided, which favours a weakening of the Iceland low pressure system. Under these circumstances, a significant weakening of the Azores high is also found if the CP El Niño is "strong" (200% CP events). In these cases, an anomalous negative NAO-like pattern is identified.

Regarding La Niña events a weaker impact, compared to that of El Niño events, is detected over the NAE sector. Opposite SLP signatures, at high and subtropical latitudes, are found for the same La Niña pattern over the North Atlantic depending on the SST background state. If the tropical Pacific SST background conditions are warmer than usual, a stronger anomalous convergence is detected in the upper troposphere when a La Niña pattern is superimposed. Under these

circumstances the Rossby wavetrain associated with the La Niña forcing is modified, and the zonal and thermally driven Walker cell connecting the Pacific and the Atlantic basins is enhanced. These characteristics associated with CP La Niñas are broadly reproduced for EP La Niñas, just finding slight differences in the intensity and spatial location of some centers of action (see Figure A2 of supplementary material). According to the results presented here, the positive NAO-like pattern usually related to La Niña events (Fraedrich and Müller, 1992; Gouirand and Moron, 2003; Moron and Plaut, 2003; Moron and Gouirand, 2003; Pozo-Vázquez et al, 2001, 2005b) could take place only during selected decades.

As this study is based on idealised experiments, a basic validation of the distinct model mean responses obtained is recommended in order to put our results in context with the observations. To this aim, SLP composites maps over the NAE sector are calculated in the observational period for each ENSO forcing and ocean mean states (Figure 8). This composite analysis is based on composites of anomalies calculated for warm and cold ENSO events, being characterised the EP and CP episodes by the Niño3 and Niño4 indices, respectively. For EP Niños, the three centres of action identified in our simulations over Florida, the Labrador Strait, and the British Islands in relation to a wavetrain coming from the Eastern Pacific under a P SST mean state (Figure 3a), are also obtained in observations for those decades under a P-like SST mean state configuration (Figure 8a). Under N SST mean conditions this SLP structure is weakened for both, model (Figure 3c) and observation (Figure 8d). For CP Niños, a dipolar pattern resembling a negative NAO-like structure is found, but with different amplitudes, in P and N (Figure 8b and 8e). This feature is also coherent with the model response to CP Niños (Figures 5a and 5c). Finally, for CP Niñas, a positive NAO-like signature is detected in P for both, observations (Figure 7a) and model (Figure 8c); whilst the same is not found in N for any of them (Figures 7c and 8f). It is necessary to note that the comparison between observational and model results is far to be direct, as in the former case significant differences in ENSO forcing appears between P and N (see Figure A4 of supplementary material) and hence, to associate a distinct response over the NAE sector with an effective modulation by the SST mean state rather than with the differences in the forcing itself, is highly complicated. In spite of this aspect, as it is shown in Figure 8, the main observational characteristics identified in the ENSO-related responses in P and N mean states are consistent with those detected in model results. Two different observational SLP databases are used, finding for both of them consistent results with our experimental responses. We can conclude that the observational dependence of ENSO response over the NAE sector on the SST background conditions is, therefore, properly reproduced by the ACCESS model.

Regarding rainfall, it has been demonstrated how the dependence of ENSO signature in European rainfall on the ocean mean state is evident for EP El Niños, in agreement with previous observational studies (Mariotti et al, 2002; Knippertz et al, 2003; López-Parages and Rodríguez-Fonseca, 2012; López-Parages et al, 2014). This feature takes place even though 1) no SST anomalies over the TNA are prescribed in our simulations, and 2) the ocean-atmosphere feedbacks over the TNA, which could enhance the ENSO-related atmospheric response over the NAE (Mathieu et al, 2004), are absent in our experimental design. The other ENSO events (CP El Niños, EP La Niñas, and CP La Niñas) present a less evident dependence of European and mediterranean rainfall response to ENSO on the SST

mean state than EP El Niños. This fact could be partially explained by the aforementioned decoupling over the TNA region in our experimental design. Indeed, an eastward displacement of the centres of action associated with ENSO towards the European continent is expected if the influence associated with the TNA SSTs would be considered (Sung et al, 2013; Ham et al, 2014). Thus, further experiments, in which the anomalous SSTs over the TNA are prescribed, or in which the slab ocean model is also applied over the Atlantic basin, could shed light on new changing processes related to the non-stationary ENSO-NAE teleconnection identified in observations.

Along this study the importance of having a changing propagation of Rossby wavetrains associated with ENSO for a non-stationary impact downstream over the North Atlantic, has been highlighted. Related to this it is necessary to note the relevance of the eastern North American region for North Atlantic storm track development. According to this, the slight differences detected here in the propagation of Rossby wavetrains could induce strong changes in baroclinicity and low level heat fluxes over Newfoundland and its surrounding areas. As a consequence, the growth conditions of tropospheric eddies could be remarkably different and so, the storm track activity over the whole North Atlantic.

The present study demonstrates how the remote impact of both warm and cold ENSO events, on the NAE climate could be noticeable different depending on the low frequency variability of the SST. According to our results a warmer than usual SST background of the tropical Pacific, together with a colder than usual SST background over the North Atlantic, favours the link between ENSO and the NAE sector in twofold: 1) changing the thermally driven direct circulation (Walker and Hadley cells), and 2) varying the Rossby waves pathway in their propagation from the tropical Pacific to the North Atlantic. However, the underlying mechanism in the latter case is still unclear, needing further analysis to completely understand by which way the ocean mean state could alter the propagation of the planetary waves triggered by ENSO, in the upper troposphere. It is important to note how most of the available studies consider the jet streams as important agents controlling the propagation of Rossby waves from tropical to extratropical latitudes (Hoskins and Karoly, 1981; Hoskins and Ambrizzi, 1993; Ambrizzi et al, 1995; Branstator, 2002). Hence, the influence that changes in the ocean mean state exert on the zonal mean flow at upper levels is a matter which should be examined in detail in the future. Another interesting question emerging from this modelling study is the important role that tropical Pacific SST background state seems to play in remote ENSO responses. It should be pointed out that the SST mean state pattern prescribed in our sensitivity experiments, which is based on the changing impact of ENSO on the leading Euro-Mediterranean rainfall mode in the observational record, has strong similarities with the AMO spatial signature over both, the Atlantic and the tropical Pacific basins. According to this, one might well wonder why the non-stationary teleconnection identified in observations evolve in phase with the AMO instead of with other multidecadal variability modes associated with the Pacific SSTs such as the Pacific Decadal Oscillation (Mantua et al, 1997) or the Interdecadal Pacific Oscillation (Zhang et al, 1997). Future studies should investigate this issue and its possible relation to the model bias. Furthermore, it should be also pointed out that the distinct SST mean states prescribed in our sensitivity experiments could interact in different ways with the ENSO forcing. Which specific ENSO-related processes depend on the ocean mean state? To address this question the

non-linear interaction between the background state and the forcing must be also thoroughly analysed in forthcoming studies.

The main conclusion of our work is that the assumption of stationarity that is common to many studies of ENSO teleconnections must be clearly questioned. According to our results, impacts over the NAE sector associated with ENSO events (with different signs, patterns, and amplitudes) could be significantly different if they take place under distinct background conditions. As a consequence, the comparability between those studies considering different climatologies is limited, which could explain the apparent disagreement among them in the available literature.

Acknowledgements This work was supported by the National Spanish projects: TRACS (CGL2009-10285) and MULCLIVAR (CGL2012-38923-C02-01). In particular, JLP thanks the FPI grant (BES-2010-042234) associated with TRACS project. JLP also thanks the Monash Weather and Climate group of Monash University (Melbourne) for scientific discussions and incredible hospitality. The sensitivity experiments described in this paper were performed on Monash University.

References

Ambrizzi T, Hoskins BJ, Hsu HH (1995) Rossby Wave Propagation and Teleconnection Patterns in the Austral Winter. J. Atmos. Sci.52:3661–3672, DOI 10.1175/1520-0469(1995)0523661:RWPATP 2.0.CO;2

Barnston A, Livezey R (1987) Classification, Seasonality and Persistence of Low-Frequency Atmospheric Circulation Patterns. Mon. Wea. Rev.115:1083, DOI 10.1175/1520-0493(1987)1151083:CSAPOL 2.0.CO;2

Bi D, Dix M, Marsland SJ, OFarrell S, Rashid H, Uotila P, Hirst A, Kowalczyk E, Golebiewski M, Sullivan A, et al (2013) The access coupled model: description, control climate and evaluation. Aust Meteorol Oceanogr J 63(1):41–64

Bladé I, Newman M, Alexander MA, Scott JD (2008) The Late Fall Extratropical Response to ENSO: Sensitivity to Coupling and Convection in the Tropical West Pacific. J. Climate21:6101, DOI 10.1175/2008JCLI1612.1

Branstator G (2002) Circumglobal Teleconnections, the Jet Stream Waveguide, and the North Atlantic Oscillation. J. Climate15:1893–1910, DOI 10.1175/1520-0442(2002)0151893:CTTJSW 2.0.CO;2

Brönnimann S (2007) Impact of El Niño-Southern Oscillation on European climate. Rev. Geophys.45:RG3003, DOI 10.1029/2006RG000199

Bulić IH, Kucharski F (2012) Delayed ENSO impact on spring precipitation over North/Atlantic European region. Climate Dyn.38(11-12):2593–2612

Cassou C, Terray L (2001) Oceanic Forcing of the Wintertime Low-Frequency Atmospheric Variability in the North Atlantic European Sector: A Study with the ARPEGE Model. J. Climate14:4266–4291, DOI 10.1175/1520-0442(2001)0144266:OFOTWL 2.0.CO;2

Choi J, An SI, Kug JS, Yeh SW (2011) The role of mean state on changes in El Niño's flavor. Climate Dyn.37:1205–1215, DOI 10.1007/s00382-010-0912-1

Compo GP, Whitaker JS, Sardeshmukh PD, Matsui N, Allan RJ, Yin X, Gleason BE, Vose RS, Rutledge G, Bessemoulin P, Brönnimann S, Brunet M, Crouthamel RI, Grant AN, Groisman PY, Jones PD, Kruk MC, Kruger AC, Marshall GJ, Maugeri M, Mok HY, Nordli Ø, Ross TF, Trigo RM, Wang XL,

Woodruff SD, Worley SJ (2011) The Twentieth Century Reanalysis Project. Quart. J. Roy. Meteor. Soc.137:1–28, DOI 10.1002/qj.776

Davies T, Cullen M, Malcolm A, Mawson M, Staniforth A, White A, Wood N (2005) A new dynamical core for the Met Office's global and regional modelling of the atmosphere. Quart. J. Roy. Meteor. Soc.131(608):1759–1782

Dommenget D (2010) The slab ocean El Niño. Geophys. Res. Lett.37:L20701, DOI 10.1029/2010GL044888

Dommenget D, Latif M (2002) Analysis of observed and simulated SST spectra in the midlatitudes. Climate Dyn.19:277–288, DOI 10.1007/s00382-002-0229-9

Dommenget D, Bayr T, Frauen C (2013) Analysis of the non-linearity in the pattern and time evolution of El Niño southern oscillation. Climate Dyn.40:2825–2847, DOI 10.1007/s00382-012-1475-0

Dong B, Sutton RT, Scaife AA (2006) Multidecadal modulation of El Niño-Southern Oscillation (ENSO) variance by Atlantic Ocean sea surface temperatures. Geophys. Res. Lett.33:L08705, DOI 10.1029/2006GL025766

Fraedrich K, Müller K (1992) Climate anomalies in Europe associated with ENSO extremes. Int. J. Climatol.12:25–31, DOI 10.1002/joc.3370120104

Frauen C, Dommenget D (2010) El Niño and La Niña amplitude asymmetry caused by atmospheric feedbacks. Geophys. Res. Lett.37:L18801, DOI 10.1029/2010GL044444

Frauen C, Dommenget D, Tyrrell N, Rezny M, Wales S (2014) Analysis of the Nonlinearity of El Niño-Southern Oscillation Teleconnection. J. Climate27:6225, DOI 10.1175/JCLI-D-13-00757.1

García-Serrano J, Rodríguez-Fonseca B, Bladé I, Zurita-Gotor P, de La Cámara A (2011) Rotational atmospheric circulation during North Atlantic-European winter: the influence of ENSO. Climate Dyn.37:1727–1743, DOI 10.1007/s00382-010-0968-y

Gill AE (1980) Some simple solutions for heat-induced tropical circulation. Quart. J. Roy. Meteor. Soc.106:447–462, DOI 10.1002/qj.49710644905

Gouirand I, Moron V (2003) Variability of the impact of El Niño-Southern Oscillation on sea-level pressure anomalies over the North Atlantic in January to March(1874-1996). Int. J. Climatol.23:1549–1566, DOI 10.1002/joc.963

Graham NE, Barnett TP (1987) Sea Surface Temperature, Surface Wind Divergence, and Convection over Tropical Oceans. Science 238:657–659, DOI 10.1126/science.238.4827.657

Greatbatch RJ, Lu J, Peterson KA (2004) Nonstationary impact of ENSO on Euro-Atlantic winter climate. Geophys. Res. Lett.31:L02208, DOI 10.1029/2003GL018542

Ham YG, Sung MK, An SI, Schubert SD, Kug JS (2014) Role of tropical atlantic SST variability as a modulator of El Niño teleconnections. Asia. Pac. J. Atmos. Sci.50:247–261, DOI 10.1007/s13143-014-0013-x

Honda M, Nakamura H, Ukita J, Kousaka I, Takeuchi K (2001) Interannual Seesaw between the Aleutian and Icelandic Lows. Part I: Seasonal Dependence and Life Cycle. J. Climate14:1029–1042, DOI 10.1175/1520-0442(2001)0141029:ISBTAA 2.0.CO;2

Hoskins BJ, Ambrizzi T (1993) Rossby Wave Propagation on a Realistic Longitudinally Varying Flow. J. Atmos. Sci.50:1661–1671, DOI 10.1175/1520-0469(1993)0501661:RWPOAR 2.0.CO;2

583 Hoskins BJ, Karoly DJ (1981) The Steady Linear Response of a Spherical Atmo-
584 sphere to Thermal and Orographic Forcing. J. Atmos. Sci.38:1179–1196, DOI
585 10.1175/1520-0469(1981)0381179:TSLROA 2.0.CO;2
586 Kang IS, Kug JS (2002) El Niño and La Niña sea surface temperature anomalies:
587 Asymmetry characteristics associated with their wind stress anomalies. J. Geo-
588 phys. Res. Atmos.107:4372, DOI 10.1029/2001JD000393
589 Kang IS, No Hh, Kucharski F (2014) ENSO Amplitude Modulation Associated
590 with the Mean SST Changes in the Tropical Central Pacific Induced by At-
591 lantic Multidecadal Oscillation. J. Climate27:7911–7920, DOI 10.1175/JCLI-D-
592 14-00018.1
593 Kao HY, Yu JY (2009) Contrasting Eastern-Pacific and Central-Pacific Types of
594 ENSO. J. Climate22:615, DOI 10.1175/2008JCLI2309.1
595 Karoly DJ, Plumb RA, Ting M (1989) Examples of the Horizontal Propaga-
596 tion of Quasi-stationary Waves. J. Atmos. Sci.46:2802–2811, DOI 10.1175/1520-
597 0469(1989)0462802:EOTHPO 2.0.CO;2
598 Knight JR, Allan RJ, Folland CK, Vellinga M, Mann ME (2005) A signature
599 of persistent natural thermohaline circulation cycles in observed climate. Geo-
600 phys. Res. Lett.32:L20708, DOI 10.1029/2005GL024233
601 Knippertz P, Ulbrich U, Marques F, Corte-Real J (2003) Decadal changes in the
602 link between El Niño and springtime North Atlantic oscillation and European-
603 North African rainfall. Int. J. Climatol.23:1293–1311, DOI 10.1002/joc.944
604 Kucharski F, Ikram F, Molteni F, Farneti R, Kang IS, No HH, King M, Giuliani
605 G, Mogensen K (2015) Atlantic forcing of Pacific decadal variability. Climate
606 Dyn.pp 1–15, DOI 10.1007/s00382-015-2705-z
607 Kug JS, Jin FF, An SI (2009) Two Types of El Niño Events: Cold Tongue El Niño
608 and Warm Pool El Niño. J. Climate22:1499, DOI 10.1175/2008JCLI2624.1
609 Livezey RE, Mo KC (1987) Tropical-Extratropical Teleconnections during the
610 Northern Hemisphere Winter. Part II: Relationships between Monthly Mean
611 Northern Hemisphere Circulation Patterns and Proxies for Tropical Convec-
612 tion. Mon. Wea. Rev.115:3115, DOI 10.1175/1520-0493(1987)1153115:TETDTN
613 2.0.CO;2
614 López-Parages J, Rodríguez-Fonseca B (2012) Multidecadal modulation of El Niño
615 influence on the Euro-Mediterranean rainfall. Geophys. Res. Lett.39:L02704,
616 DOI 10.1029/2011GL050049
617 López-Parages J, Rodríguez-Fonseca B, Terray L (2014) A mechanism for the mul-
618 tidecadal modulation of ENSO teleconnection with Europe. Climate Dyn.45(3-
619 4):867–880, DOI 10.1007/s00382-014-2319-x
620 Mantua NJ, Hare SR, Zhang Y, Wallace JM, Francis RC (1997) A Pa-
621 cific Interdecadal Climate Oscillation with Impacts on Salmon Pro-
622 duction. Bull. Amer. Meteor. Soc.78:1069–1079, DOI 10.1175/1520-
623 0477(1997)0781069:APICOW 2.0.CO;2
624 Mariotti A, Zeng N, Lau KM (2002) Euro-Mediterranean rainfall and
625 ENSO-a seasonally varying relationship. Geophys. Res. Lett.29:1621, DOI
626 10.1029/2001GL014248
627 Martin G, Bellouin N, Collins W, Culverwell I, Halloran P, Hardiman S, Hinton T,
628 Jones C, McDonald R, McLaren A, et al (2011) The HadGEM2 family of met
629 office unified model climate configurations. Geosci. Model. Dev. Discuss.4:765–
630 841

631 Martin GM, Milton SF, Senior CA, Brooks ME, Ineson S, Reichler T, Kim
632 J (2010) Analysis and Reduction of Systematic Errors through a Seamless
633 Approach to Modeling Weather and Climate. J. Climate23:5933–5957, DOI
634 10.1175/2010JCLI3541.1
635 Mathieu PP, Sutton RT, Dong B, Collins M (2004) Predictability of Win-
636 ter Climate over the North Atlantic European Region during ENSO Events.
637 J. Climate17:1953–1974, DOI 10.1175/1520-0442(2004)0171953:POWCOT
638 2.0.CO;2
639 Mo KC, Livezey RE (1986) Tropical-Extratropical Geopotential Height Teleconn-
640 nections during the Northern Hemisphere Winter. Mon. Wea. Rev.114:2488,
641 DOI 10.1175/1520-0493(1986)1142488:TEGHTD 2.0.CO;2
642 Moron V, Gouirand I (2003) Seasonal modulation of the El Niño-southern oscil-
643 lation relationship with sea level pressure anomalies over the North Atlantic in
644 October-March 1873-1996. Int. J. Climatol.23:143–155, DOI 10.1002/joc.868
645 Moron V, Plaut G (2003) The impact of El Niño-southern oscillation upon
646 weather regimes over Europe and the North Atlantic during boreal winter.
647 Int. J. Climatol.23:363–379, DOI 10.1002/joc.890
648 Murphy JM, Sexton DMH, Barnett DN, Jones GS, Webb MJ, Collins M, Stain-
649 forth DA (2004) Quantification of modelling uncertainties in a large ensemble
650 of climate change simulations. Nature430:768–772, DOI 10.1038/nature02771
651 Peng S, Whitaker JS (1999) Mechanisms Determining the Atmospheric Response
652 to Midlatitude SST Anomalies. J. Climate12:1393–1408, DOI 10.1175/1520-
653 0442(1999)0121393:MDTART 2.0.CO;2
654 Philip S, van Oldenborgh GJ (2009) Significant Atmospheric Nonlinearities in the
655 ENSO Cycle. J. Climate22:4014, DOI 10.1175/2009JCLI2716.1
656 Pozo-Vázquez D, Esteban-Parra MJ, Rodrigo FS, Castro-Díez Y (2001) The As-
657 sociation between ENSO and Winter Atmospheric Circulation and Tempera-
658 ture in the North Atlantic Region. J. Climate14:3408–3420, DOI 10.1175/1520-
659 0442(2001)0143408:TABEAW 2.0.CO;2
660 Pozo-Vázquez D, Gámiz-Fortis SR, Tovar-Pescador J, Esteban-Parra MJ, Castro-
661 Díez Y (2005a) El Niño-southern oscillation events and associated European
662 winter precipitation anomalies. Int. J. Climatol.25:17–31, DOI 10.1002/joc.1097
663 Pozo-Vázquez D, Gámiz-Fortis SR, Tovar-Pescador J, Esteban-Parra MJ, Castro-
664 Díez Y (2005b) North Atlantic Winter SLP Anomalies Based on the Autumn
665 ENSO State. J. Climate18:97–103, DOI 10.1175/JCLI-3210.1
666 Quadrelli R, Wallace JM (2002) Dependence of the structure of the Northern
667 Hemisphere annular mode on the polarity of ENSO. Geophys. Res. Lett.29:2132,
668 DOI 10.1029/2002GL015807
669 Rayner NA, Parker DE, Horton EB, Folland CK, Alexander LV, Rowell DP,
670 Kent EC, Kaplan A (2003) Global analyses of sea surface temperature, sea
671 ice, and night marine air temperature since the late nineteenth century. J. Geo-
672 phys. Res. Atmos.108:4407, DOI 10.1029/2002JD002670
673 Ruiz-Barradas A, Carton JA, Nigam S (2003) Role of the Atmosphere in Climate
674 Variability of the Tropical Atlantic. J. Climate16:2052–2065, DOI 10.1175/1520-
675 0442(2003)016 2052:ROTAIC 2.0.CO;2
676 Sung MK, Ham YG, Kug JS, An SI (2013) An alterative effect by the tropical
677 north atlantic sst in intraseasonally varying el nino teleconnection over the north
678 atlantic. Tellus65

679 Sutton RT, Hodson DLR (2003) Influence of the Ocean on North Atlantic
680 Climate Variability 1871-1999. J. Climate16:3296–3313, DOI 10.1175/1520-
681 0442(2003)0163296:IOTOON 2.0.CO;2
682 Takaya K, Nakamura H (2001) A Formulation of a Phase-Independent Wave-
683 Activity Flux for Stationary and Migratory Quasigeostrophic Eddies on a
684 Zonally Varying Basic Flow. J. Atmos. Sci.58:608–627, DOI 10.1175/1520-
685 0469(2001)0580608:AFOAPI 2.0.CO;2
686 Toniazzo T, Scaife A (2006) The influence of ENSO on winter North Atlantic
687 climate. Geophys. Res. Lett.33:L24704, DOI 10.1029/2006GL027881
688 Trenberth KE, Paolino DA (1980) The Northern Hemisphere Sea-Level Pressure
689 Data Set: Trends, Errors and Discontinuities. Mon. Wea. Rev.108:855, DOI
690 10.1175/1520-0493(1980)1080855:TNHSLP 2.0.CO;2
691 Trenberth KE, Branstator GW, Karoly D, Kumar A, Lau NC, Ropelewski C (1998)
692 Progress during TOGA in understanding and modeling global teleconnections
693 associated with tropical sea surface temperatures. J. Geophys. Res.103:14,291,
694 DOI 10.1029/97JC01444
695 Wang C (2002a) Atlantic Climate Variability and Its Associated At-
696 mospheric Circulation Cells. J. Climate15:1516–1536, DOI 10.1175/1520-
697 0442(2002)0151516:ACVAIA 2.0.CO;2
698 Wang C (2002b) Atmospheric Circulation Cells Associated with the
699 El Niño-Southern Oscillation. J. Climate15:399–419, DOI 10.1175/1520-
700 0442(2002)0150399:ACCAWT 2.0.CO;2
701 Wang C, Enfield DB (2003) A Further Study of the Tropical Western Hemisphere
702 Warm Pool. J. Climate16:1476–1493, DOI 10.1175/1520-0442-16.10.1476
703 Wang C, Picaut J (2004) Understanding ENSO physics: a review. AGU Geophys-
704 ical Monograph Series 147:21–48, DOI 10.1029/147GM02
705 Washington WM, Meehl GA (1984) Seasonal Cycle Experiment on the Climate
706 Sensitivity Due to a Doubling of CO_2 with an atmospheric general circulation
707 model coupled to a simple mixed-layer ocean model. J. Geophys. Res.89:9475–
708 9503, DOI 10.1029/JD089iD06p09475
709 Wilks DS (2011) Statistical methods in the atmospheric sciences, vol 100. Aca-
710 demic press
711 Wu A, Hsieh WW (2004) The nonlinear association between ENSO and
712 the Euro-Atlantic winter sea level pressure. Climate Dyn.23:859–868, DOI
713 10.1007/s00382-004-0470-5
714 Zhang Y, Wallace JM, Battisti DS (1997) ENSO-like Interdecadal Variability:
715 1900-93. J. Climate10:1004–1020, DOI 10.1175/1520-0442(1997)0101004:ELIV
716 2.0.CO;2

5 Figures

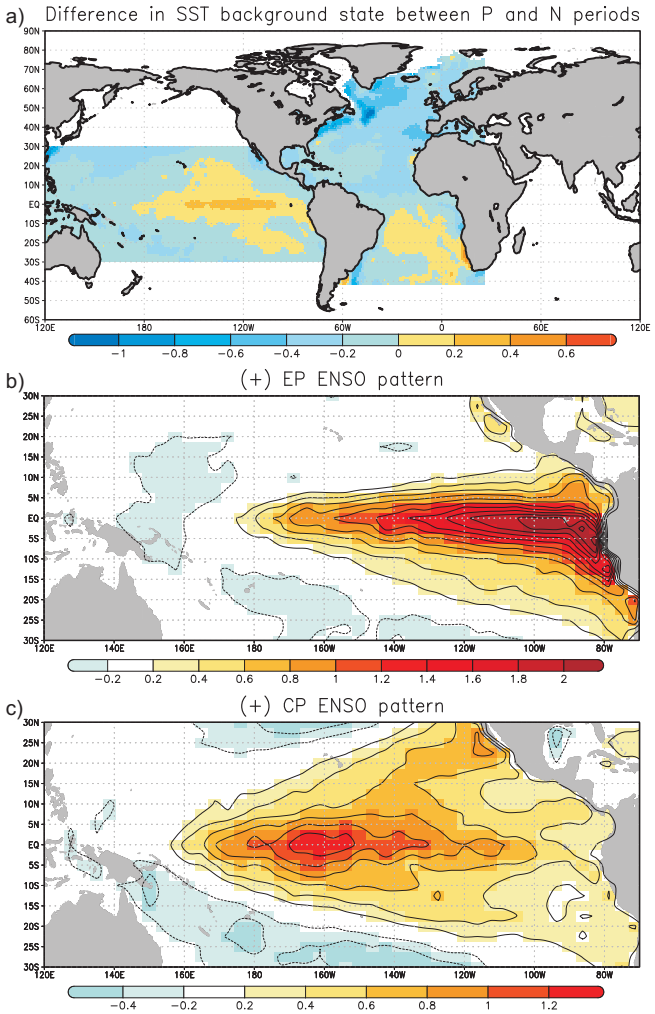

Fig. 1 a) P (1910-1940 + 1965-1990) minus N (1941-1955 + 1995-2009) Sea Surface Temperature annual mean state obtained from HadISST. Units are $[K]$ b) Standardised EP 100% ENSO pattern c) Standardised CP 100% ENSO patterns. ENSO patterns (the same as in Dommenget et al, 2013) are normalised by their corresponding SST anomalies over the El Niño34 region $[K/(KNino34)^{-1}]$. The simple slab ocean model is active outside the Atlantic and the tropical Pacific (white areas in figure above).

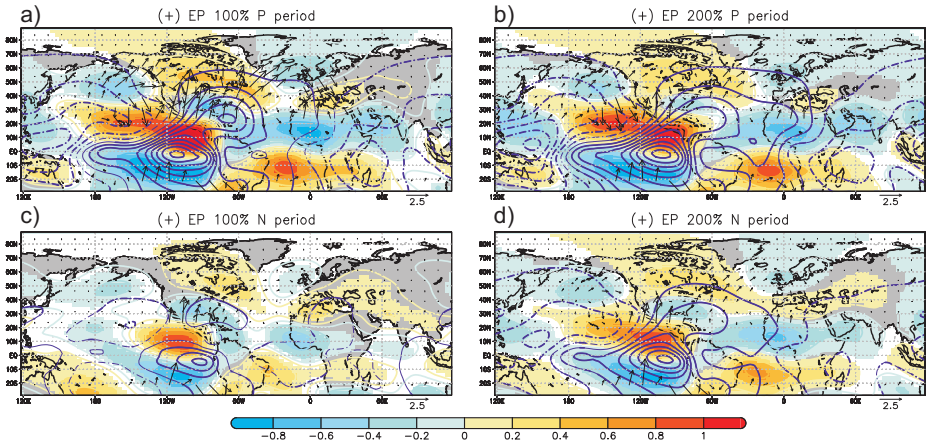

Fig. 2 EP El Niños. Streamfunction (units in $10^7 m2/s$), velocity potential (with opposite sign; $10^7 m2/s$), and wave activity flux (arrows; m^2/s^2), at upper troposphere (200hPa) under P (top) and N (bottom) mean states. On the left side, results for 100% EP ENSO amplitude. On the right side, for EP 200% amplitude. The patterns are February-March-April seasonal means normalized by the corresponding SST mean anomalies over the El Niño3.4 region (Units in K^{-1}). Only the 95% significant regions are shown for streamfunction (shaded areas). For velocity potential (purple contours) the whole signal is plotted but only the 95% significant response is bolded. The minimum (maximum) contour represented, for positive (negative) values, is $0.05 \cdot 10^7$ ($-0.05 \cdot 10^7$), with ci= $0.05 \cdot 10^7$. Only the WAF values larger than 1 m^2/s^2 are shown, being removed the values for equatorial latitudes (lower than 10).

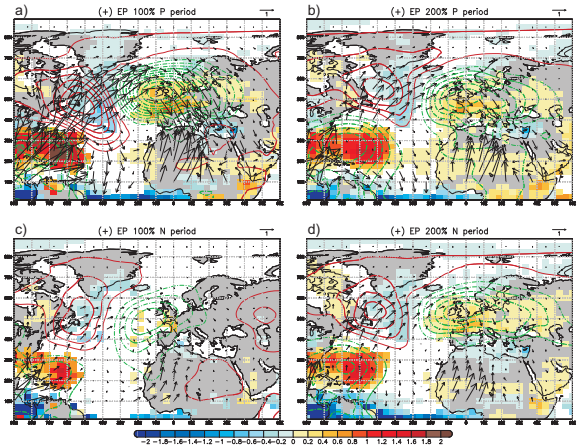

Fig. 3 EP El Niños. Rainfall (shaded; $10^{-5} Kg/m^2 s$), SLP (red and green contours for positive and negative values, respectively; Pa), and WAF (arrows; m^2/s^2), over the NAE sector under P (top) and N (bottom) mean states. On the left side, results for 100% EP ENSO amplitude. On the right side, for EP 200% amplitude. The patterns are February-March-April seasonal means normalized by the corresponding Niño3.4 mean anomalies (Units in K^{-1}). Only the 95% significant regions are shown for rainfall. For SLP (purple contours) the whole signal is plotted but only the 95% significant response is bolded. The minimum (maximum) contour represented, for positive (negative) values, is 30 (-30), with ci= 30. Only the WAF values larger than 1 m^2/s^2 are shown, being removed the values for equatorial latitudes (lower than 10).

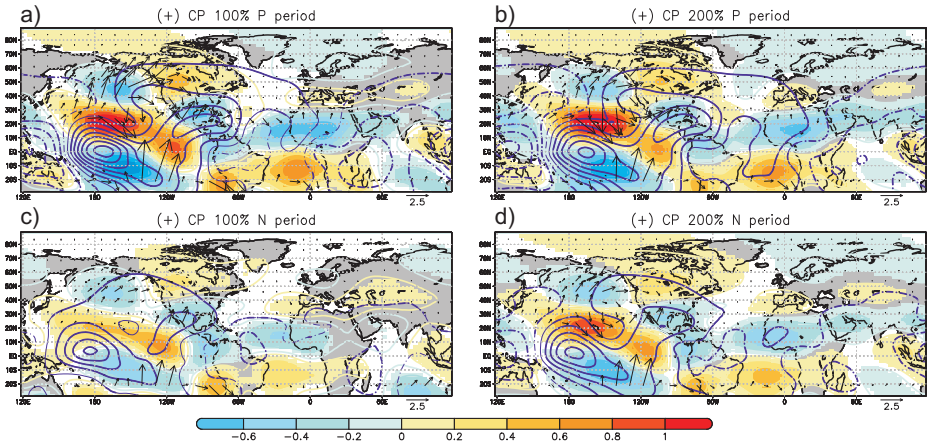

Fig. 4 CP El Niños. Same as Figure 2 but for CP El Niños.

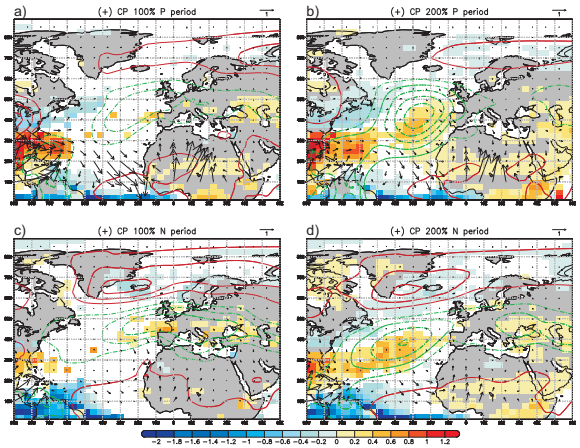

Fig. 5 CP El Niños. Same as Figure 3 but for CP El Niños.

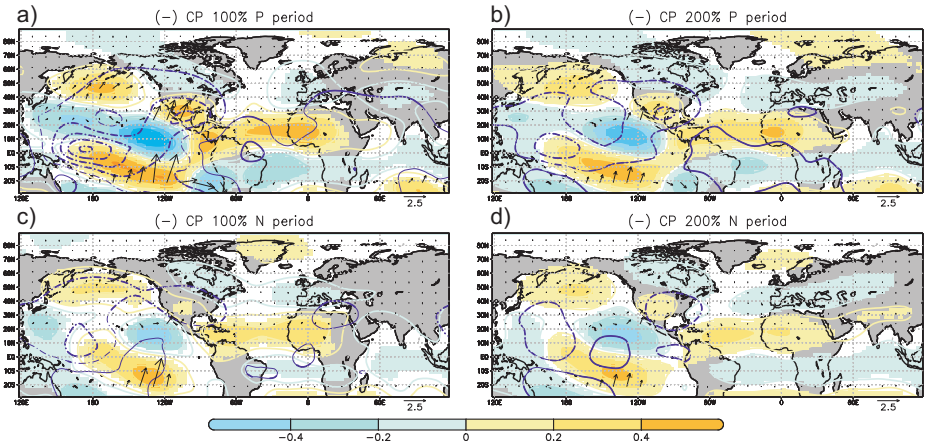

Fig. 6 CP La Niñas. Same as Figure 2 but for CP La Niñas.

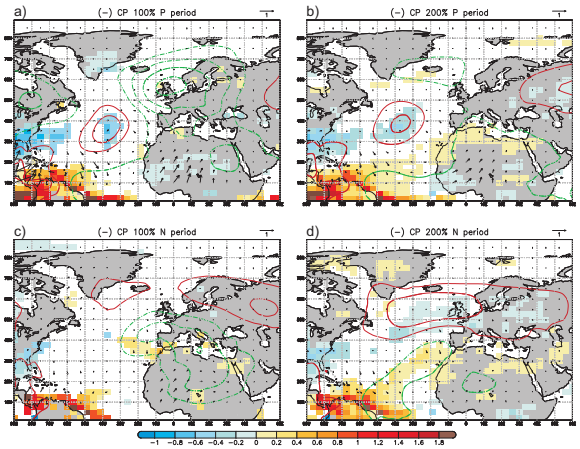

Fig. 7 CP La Niñas. Same as Figure 3 but for CP La Niñas.

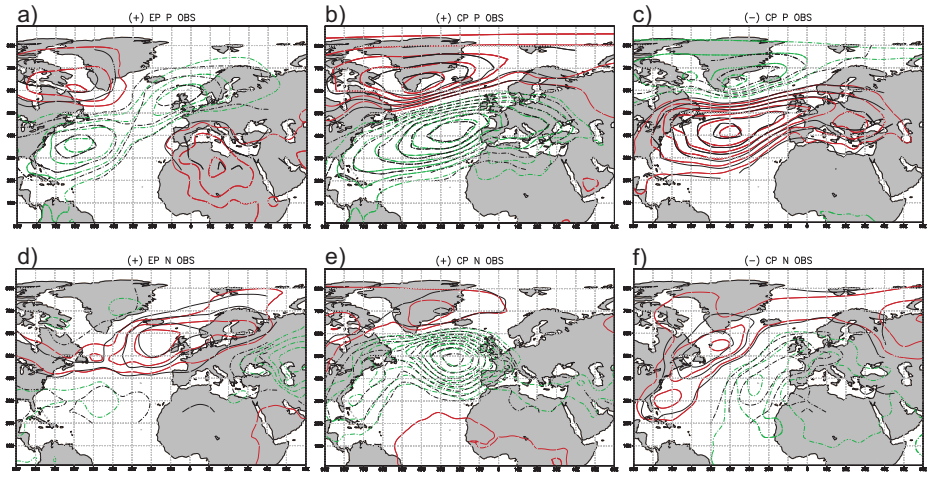

Fig. 8 Observational ENSO impact. SLP response of EP and CP ENSO over the NAE sector in P (1910-1940 and 1965-1990; top) and N (1941-1955 and 1995-2009; bottom) observational periods. They are constructed by calculating the composite maps based on those years in which the Niño3 (EP) and Niño4 (CP) indices exceeds 0.5 (-0.5 for La Niña events) standard deviations. Red (solid yellow) and green (dashed yellow) contours represent positive and negative values from 20CR (NCAR) database. The 95% significant responses are bolded. Contours lines are the same as in figures 3, 5, and 7.